crystals

MDPI

Article

Growth of Spontaneous Nucleation AlN Crystals by Al-Base Alloy Evaporation in Nitrogen Atmosphere

Xiaochun Tao, Yongkuan Xu *, Jianli Chen, Yonggui Yu, Xiaofang Qi, Wencheng Ma and Zhanggui Hu

Tianjin Key Laboratory of Functional Crystal Materials, Institute of Functional Crystals, Tianjin University of Technology, Tianjin 300384, China; taoxiaochun0203@163.com (X.T.); jlchen10@mails.jlu.edu.cn (J.C.); yuyg@email.tjut.edu.cn (Y.Y.); xfqi@ujs.edu.cn (X.Q.); wcma@email.tjut.edu.cn (W.M.); hu@tjut.edu.cn (Z.H.)
* Correspondence: xu_yk@email.tjut.edu.cn

Abstract: Aluminum nitride (AlN) crystals with areas ranging from 1 mm^2 to 2 mm^2 were successfully grown through spontaneous nucleation at 1700 °C using a modified vapor transport method. In this approach, Cu–Al alloy served as the source of aluminum (Al), and nitrogen (N_2) was employed as the nitrogen source. The morphology and crystalline quality of the AlN crystals were characterized by a stereo microscope, Raman spectrometer, photoluminescence (PL) and secondary-ion mass spectrometry (SIMS). Deposited on the graphite lid, the as-grown AlN crystals exhibited both rectangular and hexagonal shapes, identified as *m*-plane and *c*-plane AlN, respectively, based on Raman spectroscopy. The full width half maximum (FWHM) values of E_2 (high) for the rectangular and hexagonal grains were measured to be 6.00 cm^{-1} and 6.06 cm^{-1}, respectively, indicating high crystalline quality. However, PL and SIMS analysis indicated the presence of impurities associated with oxygen in the crystals. This paper elucidates the growth mechanism of the modified vapor transport method and highlights the role of the Cu–Al alloy in sustaining reactions at lower temperatures. The addition of copper (Cu) not only facilitates sustainable reactions, but also provides a novel perspective for the growth of AlN single crystals.

Keywords: flux alloy; vapor transport; AlN crystals; spontaneous nucleation

Citation: Tao, X.; Xu, Y.; Chen, J.; Yu, Y.; Qi, X.; Ma, W.; Hu, Z. Growth of Spontaneous Nucleation AlN Crystals by Al-Base Alloy Evaporation in Nitrogen Atmosphere. *Crystals* **2024**, *14*, 331. https://doi.org/10.3390/cryst14040331

Academic Editor: Francisco M. Morales

Received: 30 January 2024
Revised: 16 March 2024
Accepted: 28 March 2024
Published: 30 March 2024

1. Introduction

Aluminum nitride (AlN) has attracted extensive studies in recent years, due to its extraordinary properties, such as direct wide band gap (6.2 eV), excellent thermal conductivity, and remarkable chemical stability [1]. With an ultra-wide band gap, AlN has successfully served in the field of optoelectronics, especially in the ultraviolet range [2]. Moreover, because of its excellent thermal conductivity and electrical insulation properties, AlN is also a promising candidate for use as a heat sink material in the applications of high-power and high-frequency electronics [3]. Meanwhile, the better lattice and thermal match with other nitrides makes AlN the perfect substrate choice for the heteroepitaxial growth of III-nitrides and their alloys [4].

Several methods have been proposed for the growth of AlN bulk crystals, including physical vapor transport (PVT), the vaporization of aluminum (Al) metal, and solution routes [5–7]. Among these, PVT has been considered as the most effective method for growing AlN single crystals to date [8]. However, the conventional PVT method relies on the sublimation of AlN powder, which demands extremely high temperatures (2000–2300 °C). The strong activity of Al vapor at such temperatures usually poses challenges, leading to the corrosion and deterioration of reactor parts and crucibles [9]. Alternatively, the vaporization of Al metal in a nitrogen (N_2) atmosphere could present a promising avenue for growing AlN at lower temperatures [10].

AlN crystals with the shape of fine filaments and needles have been achieved through the nitridation of Al melt within the temperature range of 1450–1900 °C [11]. Twinned

AlN platelets have been observed within the temperature range of 1900–2100 °C, and AlN *c*-plates have also been synthesized at temperatures above 2100 °C by using BN crucibles [12]. However, the growth process is hindered by uncontrollable morphology due to the difference between the evaporation and nitridation rates of Al [13]. Since N_2 struggled to react directly with aluminum, it often requires extremely high temperatures to ensure the sufficient nitriding of Al vapor. Additionally, the prolonged reaction time also leads to a form of polycrystalline AlN shell or aggregations on the surface of the molten metal, inhibiting further Al evaporation and AlN growth [14]. Some researchers have proposed ammonia (NH_3) as a great choice for the source of N, because NH_3 is more reactive than N_2 [15]. However, NH_3 is a toxic gas, which will pollute the environment. Song et al. also obtained polyhedral crystals on the BN crucible in Al–Sn melt (Al wires and Sn grains are the origin of Al and Sn, respectively) in argon and N_2 atmosphere [16]. To overcome challenges in the growth of AlN single crystals, we propose a modified vapor transport method at relatively lower temperatures, utilizing aluminum-containing alloys as the source.

In this study, we successfully realized the spontaneous nucleation of AlN crystals on a graphite lid through the vaporization and nitridation of Cu–Al binary alloys in a graphite crucible. Notably, the solubility of AlN in copper (Cu) flux reaches from 5 mol% at 1700 °C to 20 mol% at 2000 °C [17]. This remarkable increase in AlN solubility indicates that by forming Cu–Al alloys, the nitride coating on the melt surface could be effectively suppressed during the growth and nitriding process, which is greatly beneficial for the further continuous growth of crystals. Moreover, the presence of Cu would also contribute to a reduction in the melting temperature of the binary alloy.

2. Materials and Methods

2.1. The Sintering of Al-Base Alloy

Al (99.9%, Zhong Ye Xin Dun Alloy, Beijing, China) and Cu (99.9%, Zhong Ye Xin Dun Alloy, Beijing, China) were utilized as the flux alloy. The raw materials were weighed according to the molar ratio of $Cu_{66}Al_{34}$, and then placed in a graphite crucible with a lid. The crucible was located in an induction furnace (rated power: 60 kW; operating frequency: 8 kHz). The furnace chamber was firstly filled with 30 KPa argon and then pumped to a vacuum below 1×10^{-4} Pa. The process was repeated three times in order to eliminate residual oxygen and other impurities in the furnace. After that, the furnace was filled with 1 atm argon and heated at 1500 °C for 10 h. The temperature was measured using an infrared thermometer whose minimum for measurement was 700 °C. This process allowed the raw materials to form melt flux alloys and prevented the forming of dense AlN shells on the surface of the Al.

2.2. The AlN Crystals Growth by the Modified Vapor Transport Method

After the required flux alloy was formed, the furnace was filled with 70 KPa N_2 and 30 KPa argon, and the modified vapor transport growth of AlN crystals was initialized by increasing the temperature to 800 °C. Then, the system was heated to 1700 °C at the rate of 600 °C/h, and maintained for 5 h. Subsequently, the furnace was gradually cooled to 1500 °C within 24 h and then down to 700 °C within 10 h. The rates of cooling were 8.33 °C/h and 80 °C/h, respectively. Finally, the system was naturally cooled down to room temperature. A schematic temperature diagram of the growth process is illustrated in Figure 1.

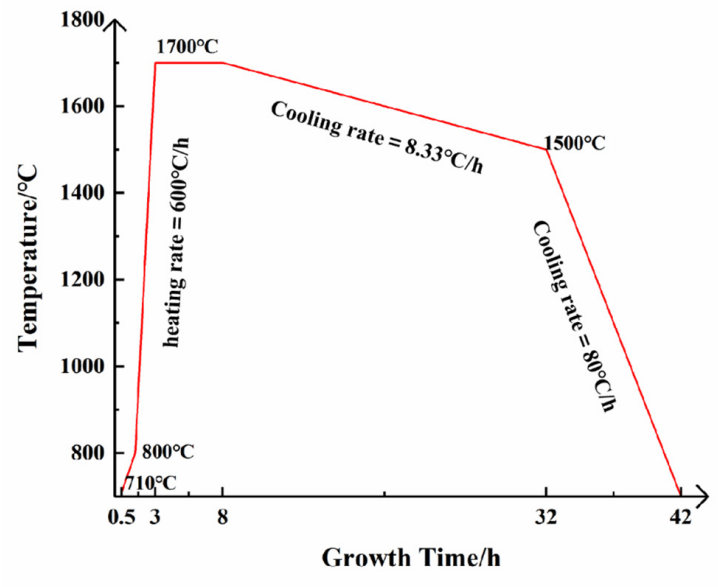

Figure 1. Schematic temperature diagram of the growth process.

2.3. The Cleanliness of AlN Crystals

When the cooling was over, the crucible lid was transferred to a Muffle furnace and kept at 300 °C for 2 h to separate the AlN crystals. The separated crystals were heated up to 600 °C and maintained for 20 h to wipe off the residue of the crucible. Then, the crystals were placed in a mixed acid solution of HF and HNO_3 (volume ratio 1:2) to remove the residual metals, and the remaining acid solution was cleaned by ultrasonic processing with deionized water. The objective of cleanliness was sought in order to better observe the surface morphology of the synthesized AlN crystals.

2.4. Characterizations

The morphology of the AlN crystals was observed using a stereoscopic optical microscope (OLYMPUS, SZ-ILST, Tokyo, Japan) and fluorescence microscope (OLYMPUS DP74, Tokyo, Japan). Raman spectra were obtained using a laser confocal Raman spectrometer (Horiba Evolution, Tokyo, Japan) with an excitation wavelength of 532 nm. The power of Raman measurements was 9 mW. The number of accumulations was 10. The integration time was 4 s. Additionally, the photoluminescence (PL) spectra were measured using a fluorescence spectrum analyzer (Edinburgh FLS-980, Livingston, UK) with a 450 W xenon arc lamp as the continuous excitation light source. The power density of PL was 1.84×10^2 W/cm^2. The excitation wavelength was 325 nm and the PL was measured at a range of 350–700 nm. The step and dwell were 1 nm and 0.500 s, respectively. Secondary-ion mass spectrometry (SIMS, CAMECA IMS 4f, Paris, France) was utilized to characterize oxygen content. SIMS profiles were obtained using a 5 keV Cs + ion beam in the negative mode.

3. Results and Discussions

3.1. Surface Morphology of Spontaneous Nucleation AlN Crystals

By adjusting the position of the crucible within the furnace, the temperature distribution and gas exchange inside the crucible could be effectively controlled. Following the growth process, a substantial number of small AlN grains emerged on the graphite crucible lid, with the majority near the center and fewer towards the edges of the graphite lid (as depicted in Figure 2). The sizes of most crystals ranged from 1 mm^2 to 2 mm^2. The crystals obtained under this temperature condition exhibited varied shapes, including rectangular crystals, hexagonal plates, as well as tilted hexagons at specific angles with the graphite lid. The distributions of these shapes were 44.12% rectangular crystals, 25% hexagonal plates, and 30.88% tilted hexagons, respectively.

Figure 2. A photograph of AlN crystals on the graphite lid after growth.

The rectangular crystal in Figure 3a (as shown by orange arrows) measures to be 1.1 mm in length and 0.8 mm in width. Noticeable growth striations parallel to the long axis on its surface have been observed (shown in Figure 3b,c, Figure 3c is a larger image of the orange area in Figure 3b), indicating a step-flow growth mode. The severely distorted region on the right side (shown in Figure 3d which is a larger image of the red area in Figure 3b) could be attributed to local strains. The upper surface of this grain is slightly narrower than the bottom, and the grain thickness is approximately 66.71 μm.

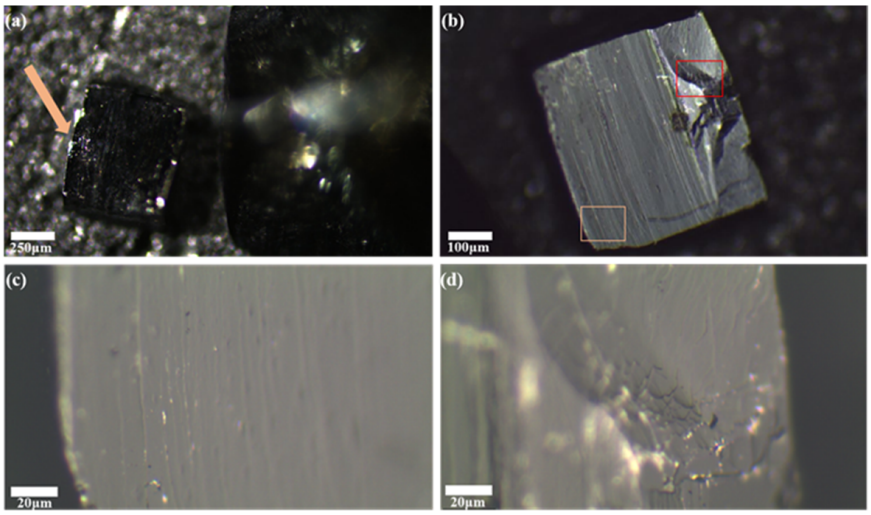

Figure 3. (**a**) Stereoscopic optical microscope photo of rectangular shaped crystal; (**b**) optical micrograph at higher magnification; (**c**,**d**) optical micrographs framed in (**b**).

The typical morphology of hexagonal crystals is depicted in Figure 4. As seen in Figure 4a, it formed a hexagonal platelet crystal with spiral marks on the surface and six-fold symmetry facets on the side, featuring a clearly visible hole (as shown in Figure 4b). Each side of the hexagon measured almost 1 mm, and the crystal had a height of 138.04 μm. In Figure 4c, a tilted hexagonal crystal at a certain angle with the graphite lid is shown,

whose sides also measured 1 mm in length. The spiral marks of the tilted hexagonal crystals are more obvious than those of hexagonal platelet crystals, as seen in Figure 4d.

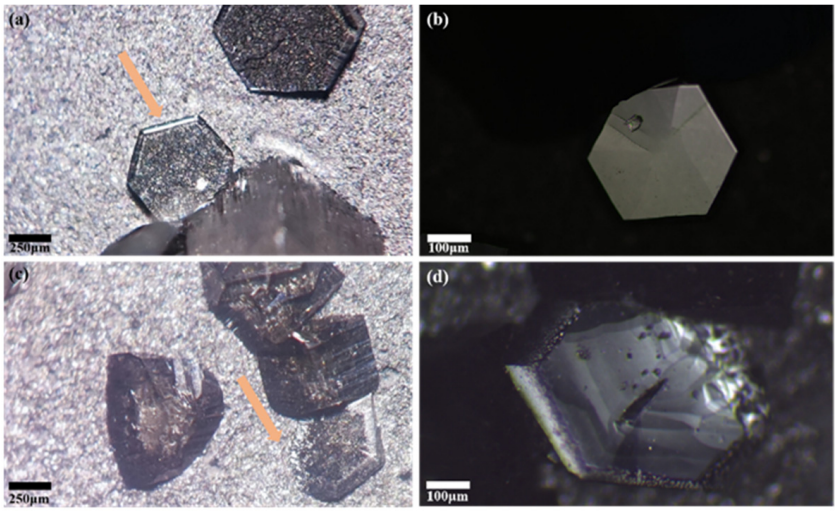

Figure 4. (**a**) Stereoscopic optical microscope photo of hexagonal platelet crystal (As shown by orange arrows); (**b**) optical micrograph at higher magnification of (**a**); (**c**) stereoscopic optical microscope photo of hexagonal crystal (As shown by orange arrows) with a certain angle of graphite and (**d**) optical micrograph at higher magnification of (**c**).

3.2. Crystalline Quality of Spontaneous Nucleation AlN Crystals

Raman spectroscopy, a powerful non-destructive and ultra-sensitive characterization tool, is often employed for the analysis of semiconductor single-crystal materials [18]. In Figure 5, the room-temperature Raman spectra of AlN crystals are displayed. Figure 5a shows the Raman spectrum of the rectangular crystals, whose E_2 (high) mode was observed at 656.83 cm^{-1}, along with an A_1 (TO) mode at 611.06 cm^{-1} and an E_1 (TO) mode at 670.37 cm^{-1}, indicating that the grain was an *m*-plane AlN crystal growing along the direction of $[10\bar{1}0]$ [19]. In Figure 5b, however, the Raman spectrum of the AlN hexagonal crystals illustrates an E_2 (low) mode at 247.50 cm^{-1}, an E_2 (high) mode at 655.37 cm^{-1}, and an A_1 (LO) mode at 888.37 cm^{-1} instead. These observations indicate that the grain was a *c*-plane AlN crystal growing along the direction of [0001] [20].

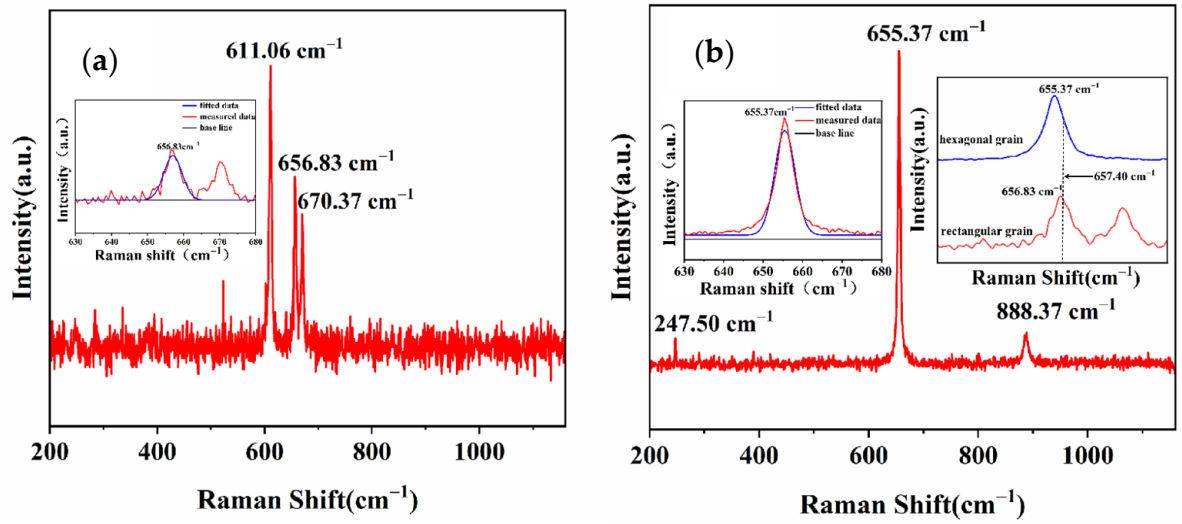

Figure 5. Raman spectra of AlN crystals with (**a**) rectangular and (**b**) hexagonal shapes. Inset: zoom on the E_2 (high) peak of fitted data, measured data and base line. Beside this, the zoom of E_2 (high) with a dashed line to show the tensile stress is shown in (**b**).

The E_2 (high) mode is highly sensitive to stress, and therefore can be utilized to analyze stress in AlN crystals [21]. Compared to the unstressed AlN crystals [22], whose E_2 (high) mode was 657.4 cm^{-1}, the E_2 (high) mode peak of the *m*-plane and *c*-plane AlN crystals were red-shifted by 0.57 cm^{-1} and 2.03 cm^{-1}, respectively, indicating that the as-grown grains had small residual tensile stress [23]. In the process of nucleation of AlN grains, the temperature gradient led to the appearance of thermal stress, which is one of the main causes of residual tensile stress inside a grain [24]. In addition, the thermal expansion coefficient mismatch between the AlN grains and graphite crucible will also lead to residual tensile stress [25].

The full width half maximum (FWHM) of E_2 (high) is a typical criterion for the evaluation of the crystal's quality [26]. By Gaussian fitting the Raman spectra (shown in the maginficaiton of E_2 (high) in Figure 5a,b), the FWHMs of the *m*- plane and *c*-plane AlN crystals are 6.00 cm^{-1} and 6.06 cm^{-1}, respectively, which are slightly larger than the self-nucleated and stress-free AlN crystals with a minimum FWHM of 3 cm^{-1} [27], indicating a further improvement that enhances the crystal's quality.

Room-temperature PL spectrum measurements were also carried out to investigate the crystalline quality of the as-grown AlN crystals, as shown in Figure 6. The characteristic PLs of rectangular and hexagonal grains are strikingly similar, exhibiting a broad emission peak between 400 and 650 nm, centered near 510 nm, which indicates the presence of a considerable number of oxygen-related impurities in the AlN crystals [28].

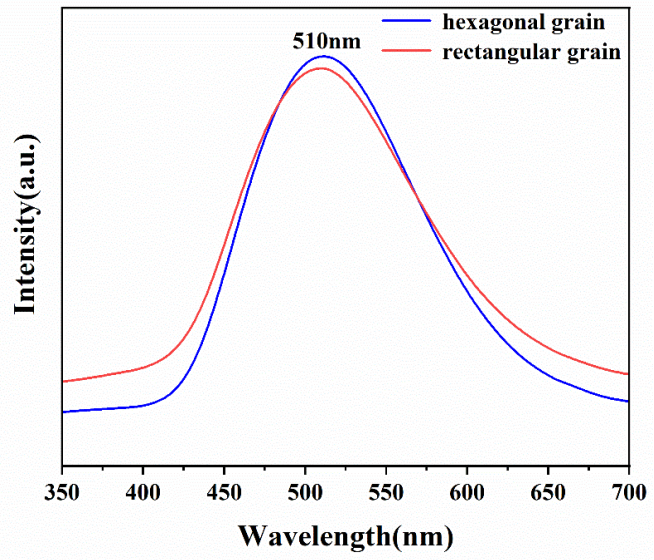

Figure 6. PL spectra of AlN crystals with rectangular (red) and hexagonal (blue) shapes.

To further investigate the presence of oxygen impurities in the AlN grains, SIMS was ultilized to measure different depths from the sample surface, as shown in Figure 7. The concentration of oxygen was measured to a level of 2.72×10^{21} cm^{-3} on the surface, and decreased exponentially until the depth reached 0.12 μm, when the oxygen level became almost constant at a level of 8.9×10^{17} cm^{-3}. As reported by Hartmann et al. [29], the AlN wafers obtained by spontaneous nucleation with the PVT method have an oxygen level of 3×10^{19} cm^{-3} and 7×10^{18} cm^{-3} in the center and edge regions, respectively. Wang et al. [30] pretreated AlN powders by three-step sintering, and the obtained AlN crystals only had an oxygen concentration of 5.6×10^{17} cm^{-3}. However, in our proposed modified vapor transport method, an Al-based alloy was used as the Al source, and the oxygen impurities in the AlN crystals may have come from the poor air tightness of the growth furnace and inadequate cleaning before growth. Given the favorable chemical affinity between aluminum and oxygen [31], the residual oxygen impurities could be dissolved into the Al–Cu alloys during the growth process, thus introducing oxygen-related impurities.

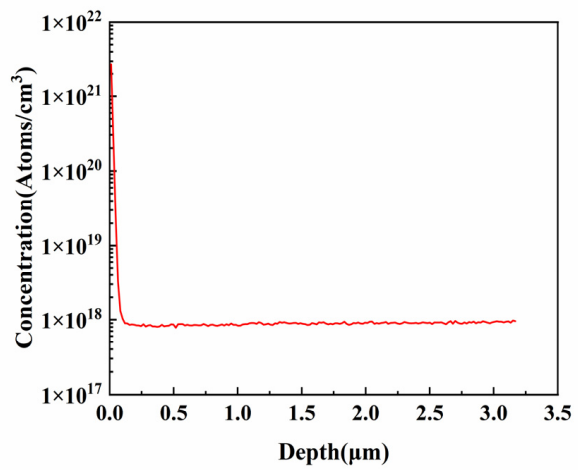

Figure 7. SIMS measurement of the oxygen in AlN crystal.

3.3. Growth Mechanism of Spontaneous Nucleation AlN Crystals

Based on the above analyses, we cans ee that the spontaneous nucleated AlN single crystals were successfully synthesized by the modified vapor transport method. Similar to PVT growth, the growth process of the modified vapor transport method could be described as follows (illustrated in Figure 8).

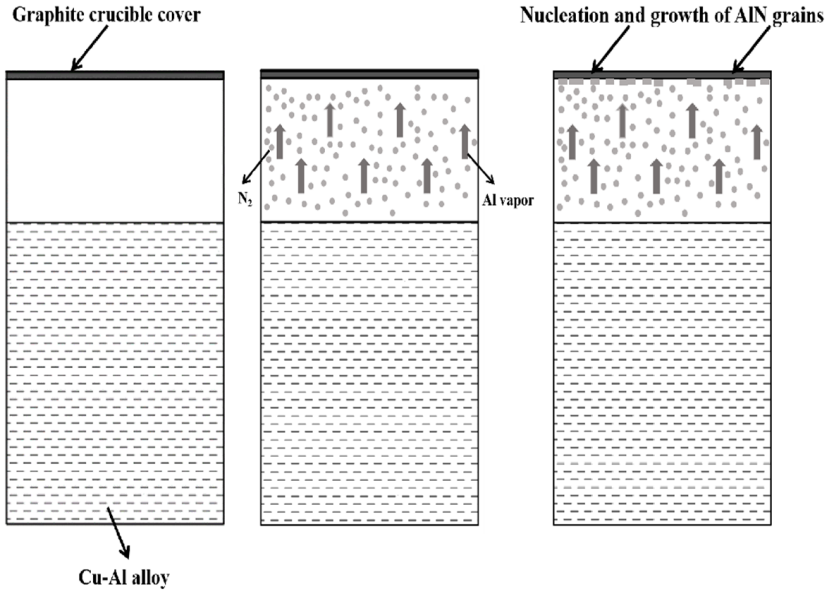

Figure 8. Schematic diagram of crystal growth using Cu–Al metals' evaporation in a N_2 atmosphere.

The first step is the formation of the gas source. The Cu–Al alloy is melted by heat, causing the aluminum to evaporate as a gas reaction source. The addition of Cu serves to reduce the melting point of the alloy, as Cu has a low saturated vapor pressure [32], which allows for controlling the evaporation rate of aluminum. Subsequently, the aluminum vapor is nitrided in a N_2 atmosphere. At the same time, nitriding also occurs on the surface of the liquid metal. The presence of Cu facilitates the dissolution of the AlN formed on the alloy surface, preventing the formation of an AlN shell and ensuring control over the aluminum evaporation rate, the nitriding rate, and the sustainability of growth. The final process involves the spontaneous nucleation and growth of AlN. Under suitable conditions, AlN crystallizes and grows on the lid due to the slow cooling process and the relatively low temperature on the crucible lid [33].

For wurtzite AlN crystals, the *c*- and *m*-planes are the two most densely packed planes in the lattice [34], and serve as growth planes for the crystals. The diffusion barrier of Al atoms on the *m*-plane is much lower along the $[11\bar{2}0]$ direction (0.11 eV) than that along the [0001] direction (2.79 eV) [35], causing a faster growth rate along the $[11\bar{2}0]$ direction. Consequently, due to such anisotropy, the *m*-plane crystal appears in a rectangular shape (as shown in Figure 9a). In the case of free growth, the *c*-plane has a six-fold symmetry, and the *c*-plane AlN crystals tend to form a hexagonal surface. However, due to the temperature gradient, vapor supersaturation, and other factors [36], the AlN crystals will also grow along directions other than [0001], and form tilted hexagons at a certain angle with the bottom, as shown in Figure 9b.

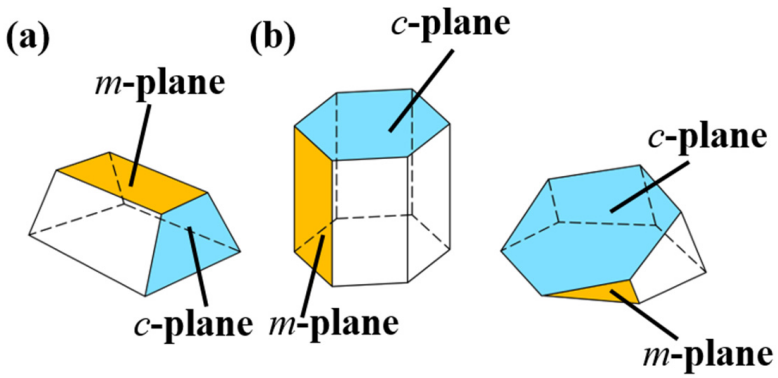

Figure 9. Schematic diagram of three shapes of crystal: (**a**) rectangular crystals, (**b**) hexagonal platelets and tilted hexagons.

4. Conclusions

AlN crystals of 1 mm^2 to 2 mm^2 have been successfully obtained through spontaneous nucleation, using Cu–Al alloy as the Al source and N_2 as the nitrogen source, via a modified vapor transport method at 1700 °C. The resulting AlN grains exhibited both rectangular and hexagonal shapes. The Raman spectra confirmed the presence of *m*-plane and *c*-plane AlN crystals, with FWHM values of E_2 (high) of 6.00 cm^{-1} and 6.06 cm^{-1}, respectively. PL analysis revealed a broad luminescence peak between 400 and 650 nm, which is associated with oxygen impurity due to the residual oxygen during the growth process. The characterization of SIMS showed that the O concentration in the AlN crystals we obtained was 8.9×10^{17} cm^{-3}. Additionally, the detailed growth mechanism and morphology origin of the crystals have been also investigated in this study. The modified vapor transport method demonstrated a sustainable growth of AlN at lower temperatures with the controllable evaporation and nitriding of Al. This approach holds promise for the prolonged and cost-effective growth of AlN single crystals, which requires further investigation.

Author Contributions: Conceptualization, Y.X.; investigation, X.T. and J.C.; resources, Y.X., Y.Y. and W.M.; data curation, X.T. and X.Q.; writing—original draft preparation, X.T.; writing—review and editing, J.C.; supervision, Z.H.; project administration, Y.X. All authors have read and agreed to the published version of the manuscript.

Funding: This research was supported by the National Natural Science Foundation of China, grant No. 52302007, 51906086.

Data Availability Statement: The original contributions presented in the study are included in the article material, further inquiries can be directed to the corresponding author.

Conflicts of Interest: The authors declare no conflicts of interest.

References

1. Strite, S.; Morkoç, H. GaN, AlN, and InN: A review. *J. Vac. Sci. Technol. B* **1992**, *10*, 1237–1266. [CrossRef]
2. Grandusky, J.R.; Chen, J.; Gibb, S.R.; Mendrick, M.C.; Moe, C.G.; Rodak, L.; Garrett, G.A.; Wraback, M.; Schowalter, L.J. 270nm Pseudomorphic Ultraviolet Light-Emitting Diodes with Over 60 mW Continuous Wave Output Power. *Appl. Phys. Express* **2013**, *6*, 032101. [CrossRef]
3. Slack, G.A.; Bartram, S.F. Thermal Expansion of Some Diamondlike Crystals. *J. Appl. Phys.* **1975**, *46*, 89–98. [CrossRef]
4. Kneissl, M.; Yang, Z.; Teepe, M.; Knollenberg, C.; Schmidt, O.; Kiesel, P.; Johnson, N.M.; Schujman, S.; Schowalter, L.J. Ultraviolet Semiconductor Laser Diodes on Bulk AlN. *J. Appl. Phys.* **2007**, *101*, 123103. [CrossRef]
5. Herro, Z.G.; Zhuang, D.; Schlesser, R.; Sitar, Z. Growth of AlN Single Crystalline Boules. *J. Cryst. Growth* **2010**, *312*, 2519–2521. [CrossRef]
6. Selvaduray, G.; Sheet, L. Aluminium Nitride: Review of Synthesis Methods. *Mater. Sci. Technol.* **2013**, *9*, 463–473. [CrossRef]
7. Li, S.; Adachi, M.; Ohtsuka, M.; Fukuyama, H. Synthesis of AlN Single Crystal by Solution Growth Method Using Type 430 Ferritic Stainless Steel Flux. *AIP Adv.* **2023**, *13*, 085105. [CrossRef]
8. Witzke, H.D. Über Wachstum von AIN-Einkristallen aus der Dampfphase. *Phys. Status Solidi* **2006**, *2*, 1109–1114. [CrossRef]
9. Yao, X.; Zhang, B.; Hu, H.; Wang, Y.; Kong, Z.; Wu, Y.; Shao, Y.; Hao, X. State-of-the-Art and Prospective Progress of Growing AlN Substrates by Physical Vapor Transport. *J. Cryst. Growth* **2023**, *617*, 127276. [CrossRef]
10. Drum, C.M. Axial Imperfections in Filamentary Crystals of Aluminum Nitride. I. *J. Appl. Phys.* **1965**, *36*, 816–823. [CrossRef]
11. Taylor, K.M.; Lenie, C. Some Properties of Aluminum Nitride. *J. Electrochem. Soc.* **1960**, *107*, 308–314. [CrossRef]
12. Schlesser, R.; Sitar, Z. Growth of Bulk AlN Crystals by Vaporization of Aluminum in a Nitrogen Atmosphere. *J. Cryst. Growth* **2002**, *234*, 349–353. [CrossRef]
13. Kobayashi, R.; Fukutomi, Y.; Takagi, T. Synthesis of AlN Needles by Nitridation of Al-Si Melt. *J. Ceram. Soc. Jap.* **2016**, *124*, 1161–1163. [CrossRef]
14. Wu, P.; Funato, M.; Kawakami, Y. Environmentally Friendly Method to Grow Wide-Bandgap Semiconductor Aluminum Nitride Crystals: Elementary Source Vapor Phase Epitaxy. *Sci. Rep.* **2015**, *5*, 17405. [CrossRef] [PubMed]
15. Hou, Q.; Mutharasan, R.; Koczak, M. Feasibility of Aluminium Nitride Formation in Aluminium Alloy. *Mater. Sci. Eng. A* **1995**, *195*, 121–129. [CrossRef]
16. Song, Y.; Kawamura, F.; Taniguchi, T.; Shimamura, K.; Ohashi, N. Conditions for growth of AlN single crystals in Al-Sn flux. *J. Am. Ceram. Soc.* **2018**, *101*, 876–4879. [CrossRef]
17. Yonemura, M.; Kamei, K.; Munetoh, S. Precipitation of Single Crystalline AlN from Cu-Al-Ti Solution under Nitrogen Atmosphere. *J. Mater. Sci. Mater. Electron.* **2005**, *16*, 197–201. [CrossRef]
18. Kazuma, T.; Hiroyuki, O.; Noriyuki, H.; Takeshi, K. Decomposition of the Anisotropic Strain in 3D-Sturcture GaN Layers Using Raman Spectroscopy. *Sci. Rep.* **2023**, *14*, 3330.
19. Zheng, W.; Zheng, R.; Huang, F.; Wu, H.; Li, F. Raman Tensor of AlN Bulk Single Crystal. *Photonics Res.* **2015**, *3*, 38. [CrossRef]
20. Cros, A.; Wang, J.; Demangeot, F.; Péchou, R.; Daudin, B. Splitting of the Surface Phonon Modes in Wurtzite Nanowires. *Jpn. J. Appl. Phys.* **2013**, *52*, 08JL1. [CrossRef]
21. Liu, L.; Liu, B.; Edgar, J.H.; Rajasingam, S.; Kuball, M. Raman Characterization and Stress Analysis of AlN Grown on SiC by Sublimation. *J. Appl. Phys.* **2002**, *92*, 5183–5188. [CrossRef]
22. Prokofyeva, T.; Seon, M.; Vanbuskirk, J.; Holtz, M.; Nikishin, S.A.; Faleev, N.N.; Temkin, H.; Zollner, S. Vibrational Properties of AlN Grown on (111)-Oriented Silicon. *Phys. Rev. B* **2001**, *63*, 125313. [CrossRef]
23. Kuball, M.; Hayes, J.M.; Prins, A.D.; van Uden, N.W.A.; Dunstan, D.J.; Shi, Y.; Edgar, J.H. Raman Scattering Studies on Single-Crystalline Bulk AlN under High Pressures. *Appl. Phys. Lett.* **2001**, *78*, 724–726. [CrossRef]
24. Wang, Q.; Huang, J.; Wang, Z.; He, G.; Lei, D.; Gong, J.; Wu, L. Anisotropic Three-Dimensional Thermal Stress Modeling and Simulation of Homoepitaxial AlN Single Crystal Growth by the Physical Vapor Transport Method. *Cryst. Growth Des.* **2018**, *18*, 2998–3007. [CrossRef]
25. Payman, K.; Antoinette, M.M. Modeling micromechanical response to thermal history in bulk grown aluminum nitride. *Phys. Status Solidi C* **2015**, *12*, 345–348.
26. Kuball, M.; Hayes, J.M.; Shi, Y.; Edgar, J.H.; Prins, A.D.; van Uden, N.W.A.; Dunstan, D.J. Raman Scattering Studies on Single-Crystalline Bulk AlN: Temperature and Pressure Dependence of the AlN Phonon Modes. *J. Cryst. Growth* **2001**, *231*, 391–396. [CrossRef]
27. Sarua, A.; Kuball, M.; Van Nostrand, J.E. Deformation Potentials of the E_2(high) Phonon Mode of AlN. *Appl. Phys. Lett.* **2002**, *81*, 1426–1428. [CrossRef]
28. Akiyama, T.; Nakamura, K.; Ito, T. Ab Initio-Based Study for Adatom Kinetics on AlN (0001) Surfaces during Metal-Organic Vapor-Phase Epitaxy Growth. *Appl. Phys. Lett.* **2012**, *100*, 251601. [CrossRef]
29. Hartmann, C.; Wollweber, J.; Dittmar, A.; Irmscher, K.; Kwasniewski, A.; Langhans, F.; Neugut, T.; Bickermann, M. Preparation of Bulk AlN Seeds by Spontaneous Nucleation of Freestanding Crystals. *Jpn. J. Appl. Phys.* **2013**, *52*, 8JA06. [CrossRef]
30. Wang, Z.; Zhu, X.; Zhao, Q.; Wu, J.; Yu, T. Oxygen Reduction Through Specific Surface Area Control of AlN Powder for AlN Single-Crystal Growth by Physical Vapor Transport. *Semicond. Sci. Technol.* **2024**, *39*, 025006. [CrossRef]
31. Slack, G.A.; Schowalter, L.J.; Morelli, D.; Freitas, J.A. Some Effects of Oxygen Impurities on AlN and GaN. *J. Cryst. Growth* **2002**, *246*, 287–298. [CrossRef]

32. Kamei, K.; Shirai, Y.; Tanaka, T.; Okada, N.; Yauchi, A.; Amano, H. Solution Growth of AlN Single Crystal Using Cu Solvent under Atmospheric Pressure Nitrogen. *Phys. Status Solidi C* **2007**, *4*, 2211–2214. [CrossRef]
33. Chen, W.; Qin, Z.; Tian, X.; Zhong, X.; Sun, Z.; Li, B.; Zheng, R.; Guo, Y.; Wu, H. The Physical Vapor Transport Method for Bulk AlN Crystal Growth. *Molecules* **2019**, *24*, 1562. [CrossRef] [PubMed]
34. Drum, C.M.; Mitchell, J.W. Electron Microscopic Examination of Role of Axial Dislocations in Growth of AlN Whiskers. *Appl. Phys. Lett.* **1964**, *4*, 164–165. [CrossRef]
35. Jindal, V.; Shahedipour-Sandvik, F. Density Functional Theoretical Study of Surface Structure and Adatom Kinetics for Wurtzite AlN. *J. Appl. Phys.* **2009**, *105*, 084902. [CrossRef]
36. Li, J.; Hu, X.; Jiang, S.; Ning, L.; Wang, Y.; Chen, X.; Xu, X.; Wang, J.; Jiang, M. Relationship between Appearance Crystalline Planes and Growth Temperatures during Sublimation Growth of AlN Crystals. *J. Cryst. Growth* **2006**, *293*, 93–96. [CrossRef]